



EFFECT OF FILM THICKNESS ON THE TRIBO-MECHANICAL PROPERTIES OF CHROME-GOLD THIN FILMS

Corina BIRLEANU¹, Marius PUSTAN¹, Violeta Valentina MERIE², Horea George CRIȘĂN¹

¹ Technical University from Cluj-Napoca, Mechanical Systems Engineering Department, Micro & Nano Systems Laboratory, 103-105 Muncii Blvd., 400641, Cluj-Napoca, Romania

² Technical University from Cluj-Napoca, Materials Science and Engineering Department, 103-105 Muncii Blvd., 400641, Cluj-Napoca, Romania

Corresponding author: Corina BIRLEANU, E-mail: Corina.Barleanu@omt.utcluj.ro

Abstract. In this paper we took into consideration two approaches in order to develop a fundamental understanding of the influence of thin film thickness on the tribological and mechanical properties of chromium-gold thin films, deposited onto a silicon substrate in terms of implementing them in reliable MEMS structures. First, the atomic force microscopy was used to quantitatively measure both the adhesion and friction forces between tip and samples and their dependence on the films thickness. Secondly, the indentation technique was used to determine the mechanical properties of chrome-gold films dependence on thickness. We concentrated on chrome-gold thin films since this alloy in bulk is known as a stable low resistance material. Due to their superior tribological properties, chrome-gold thin films have offered opportunities in many technical applications, such as protective coatings and wear-resistant coatings. The mechanical properties of chrome-gold thin films are found to be dependent on the thin films thickness. For this purpose, the experiments were focused on the mechanical and tribological investigations of chromium-gold thin films, with the thickness between 100 nm and 500 nm.

Key words: Chrome-Gold thin films, adhesion force, friction force, nano-indentation.

1. INTRODUCTION

Gold thin films due to their unique electrical and thermal conductivity, combined with high oxidation resistance, are commonly used in the microelectromechanical systems (MEMS) industry. This area is becoming more sophisticated and more competitive and designers require to push the limits of materials behavior. Even if the properties of the gold thin films are attractive, mechanical properties are often not quite ideal [1]. Thus, correlating the microstructure with material properties requires two things: a testing method able to determine the differences between materials and a controlled variation of the processing [2].

With the advancements in nanomaterial research, new thin film systems often only a few 100's of nm are being developed to improve the performance of thin coatings in all technological important areas [3-6]. Metal films properties are sensitive not only to their structures but also to many other parameters, including the technological process, deposition conditions, substrates onto which they are deposited and most essentially on their thickness [7].

In this paper we have focused on the tribo-mechanical properties of the Chromium-Gold thin film with the scope to identify the thickness effect on its properties. The work is driven by applications of thin films as contact materials for MEMS devices that are subject to multiple metal-to-metal contact and which ultimately lead to the failure of the device operation. We concentrated on Chromium-Gold films since this alloy in bulk is known as a stable low-resistance material. Due to their superior tribological properties, Chromium-Gold thin films have been proposed also to prevent stiction and to reduce friction.

One of the important aspects of thin film microstructures is the small size of the grains with effect on the mechanical properties. Thus, based on the Hall-Petch relation, the hardness and strength of films increases as the grain size decreases [8].

Chau and al. showed that in order to get the relation between pattern surface / surface chemistry due to the influence of thin film thickness it is important to comprehensively evaluate the behavior of nanofriction and adhesion effect of thin films [9, 10].

A suitable strategy for optimizing wear resistance for thin films is to maximize the H/E ratio where H is the hardness and E is the modulus of elasticity. In order to determine the H and E properties the nanoindentation method is advantageous. The performance of micro – and nano – devices depends on the surface and interface between thin film and substrate which are characterized by properties such as chemical composition, roughness, friction, adhesion, wear and so on [6, 11, 12].

The role of the high hardness, MEMS switches for example, was captured by Gregori and Clarke with two parameters, a plasticity index ψ and an adhesion parameter θ [1]. They showed that a higher hardness can minimize adhesion between contacts and protection against failure by stiction.

There are several motivations for investigating the tribological and mechanical properties of Chromium-Gold thin films. From an engineering point of view, it is necessary to evaluate the reliability of these structures because they are used in an increasing number of products.

From a scientific point of view, there is interest in understanding why the mechanical properties of these materials depend on the scale. These two objectives do not contradict each other and furthermore contribute to the scientific progress through the access provided to the experimental data collected during microscopic testing [13].

Most often, when the mechanical and tribological properties are needed, the bulk properties are adopted; therefore, the mechanical and tribological properties of thin films need to be measured accurately.

The work of this paper is divided into two segments. On the one hand, the atomic force microscopy (AFM) was used to quantitatively measure both the adhesion and friction forces between tips and sample's surfaces and their dependence on the thin film thickness. On the other hand, the indentation technique was used to determine the dependence of the mechanical properties of Chromium-Gold thin films (Young Modulus and Hardness) on thickness.

2. MATERIALS AND METHODS

2.1. Investigated samples

The investigated samples consist of thin layers of chromium and gold with different thickness. Chromium is an oxygen active material leading to very stable nucleation centers on oxidized silicon [14]. For a given gold film thickness, an optimal thickness of the chromium adhesion layer was determined. The highest adhesion was reached when the chromium interlayer was about 6-10% of the gold film thickness [13]. For the investigated thin films, the three gold thicknesses film are 100, 300 and 500 nm as reported in Table 1.

Table 1

Investigated sample

Samples ^a	Sample preparation method	Coating thickness
Si/SiO ₂ /Cr/Au-sample 1	E-beam evaporation	1.7 μ m/10nm/100 nm
Si/SiO ₂ /Cr/Au-sample 2	E-beam evaporation	1.7 μ m/30nm/300 nm
Si/SiO ₂ /Cr/Au-sample 3	E-beam evaporation	1.7 μ m/50nm/500 nm

^a The thickness of Si wafers can vary between 356–525 μ m range depending on the provider

The thin film samples were deposited at the National Institute for Research and Development in Microtechnologies, IMT- Bucharest, Romania. Electron beam evaporation (E-beam evaporation) technique involves direct film formation on a substrate surface originating from one or more vapor sources. As compared to thermal evaporation, the E-beam evaporation source uses a high energy beam of electrons to heat only a small area of the source surface, leading to high purity deposited films.

The p-type Si wafers, <100> orientation, have been used in order to prepare the experimental samples. After a standard cleaning process in piranha solution, a silicon dioxide layer with a thickness of 1.7 μm has been grown by wet oxidation of the substrate. On this layer, we have deposited two thin metal films with different thicknesses. For the first sample, we have deposited an adhesion Chromium film with a thickness of 10 nm and the gold was 100 nm thick. For the second sample, the films thickness was 30 nm for Chromium and 300 nm for gold. The last sample had the films thicknesses of 50 nm for Chromium and 500 nm for gold. The adhesion of the chromium and gold films to the substrate was evaluated using a tape test and the resistivity of the film was measured with a conventional four-point probe. The adhesion was found to be acceptable for all deposition conditions. The thickness of the coatings was measured during the deposition process by using the quartz resonator method.

2.2. Experimental procedure

The tests were performed at room temperature (22°C) and a relative humidity RH of 40% using the Atomic Force Microscope (AFM) XE-70. Each measurement was repeated 10 times in order to improve the accuracy of the experimental results. The cantilever used for tribological investigation in contact mode was HQ-NSC 35/Hard/Al BS from Si3N4 with 30 nm aluminum on the backside coating, a nominal value of the spring constant $k = 5.4 \text{ Nm}^{-1}$, the radius smaller than 20 nm and the length $l = 130 \mu\text{m}$, width $b = 35 \mu\text{m}$, thickness $g = 2 \mu\text{m}$ and height $s = 15 \mu\text{m}$. The set point was of 10 nN and the scan rate was 0.75 Hz.

The cantilever used for topography evaluation in non-contact mode was PPP-NCHR with 30 nm aluminum on the backside coating, with a nominal value of the spring constant $k = 42 \text{ Nm}^{-1}$, the radius smaller than 10 nm, resonance frequency 330 kHz, length $l = 125 \mu\text{m}$, width $b = 30 \mu\text{m}$, thickness $g = 4 \mu\text{m}$.

The nanoindentation tests were performed with a Berkovich tip with a nominal value of the spring constant $k = 144 \text{ Nm}^{-1}$, the radius smaller than 25 nm, the side angle of 79°, resonance frequency 150 kHz and geometrical parameters of the tip: height $s = 109 \mu\text{m}$, length $l = 782 \mu\text{m}$ and thickness $g = 24 \mu\text{m}$.

3. EXPERIMENTAL INVESTIGATIONS

The size effect on the strength of materials has been known as early as the 1960's and has been investigated since. Thin films generally involve two competing length scale (thickness and grain) [13]. Some materials have been sufficiently tested and the results may be regarded as 'handbook' values, i.e. they may be used in initial designs of MEMS. Such results are the goal of experimental research of this nature. In this regard, in this paper more data points for each sample were taken. This is necessary to give credence to statistical values due to variations in the material itself and the uncertainties in the measurements.

3.1. Topography

Deposited thin films look very flat macroscopically, but nonetheless possess a certain surface roughness. For evaluating the surface topography of the samples, we utilized the Non-Contact AFM mode (NC-AFM) based on the attractive inter-atomic force between the tip and the sample surface. In AFM, a sharp tip at the end of a cantilever is vibrated near the surface of a sample. Over $3 \mu\text{m} \times 3 \mu\text{m}$ surface area was scanned, which leads us to take a random area as a representative measurement for the rest of the surface. The roughness can be characterized by several parameters and functions: R_a is the arithmetic average height of roughness, R_q called root-mean-square or RMS is more sensitive to occasional highs and lows, making it a valuable complement to R_a .

When increasing the roughness, the surfaces can be more hydrophobic [9] leading to reduced capillary force and adhesion. The acquisitions of AFM images of morphologies surface and roughness surface for samples are shown in Fig. 1. Figure 1 presents typical 3D and profile images obtained with the AFM for gold 100 nm, 300 nm and 500 nm and chromium 10 nm, 30 nm and 50 nm on SiO_2 substrates. The raw images obtained using AFM techniques were treated using the associated software XEI. The surface roughness is usually represented by RMS roughness (R_q).

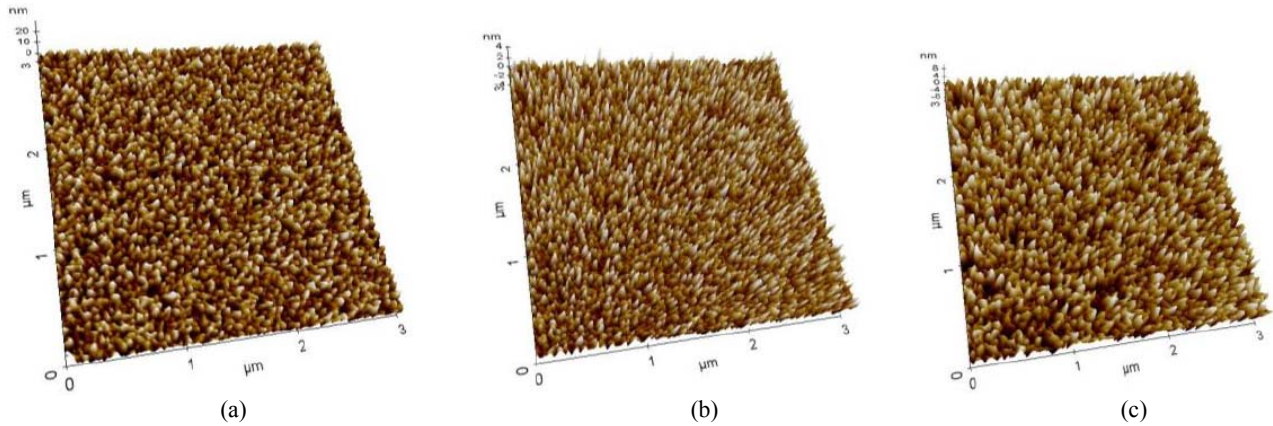


Fig. 1 – Non-contact AFM images for all three samples chromium-gold thin films with different coating thickness taken with an AFM XE-70 (3 μm x 3 μm scan size): (a) Sample 1, (b) Sample 2, (c) Sample 3.

The AFM images show the equiaxed grain structures in the deposited films. The grain size data that were obtained for the investigated films are summarized in Table 2. The results show that the average grain size of the gold samples increases with increasing film thickness from approximately 40 nm for the 100 nm thick gold film to 60 nm for 300 nm thick gold films and 80 nm for the 500 nm thick gold film. Therefore, the results are in accordance with previous studies of other thin film microstructures which show that the grains increase in size with increasing film thickness [15].

Table 2

Grain sizes obtained for the Chromium-Gold samples using AFM scans

Film thickness of gold ^a (nm)	Gold film grain size (nm)
100	38 – 41
300	57 – 59
500	78 – 82

^a The grain size of substrat varies between 29-32 nm range

In order to improve the accuracy of results, the investigated surfaces were scanned in different places, and for these measurements a statistical interpretation of the results was done by calculating the dispersion values. The average results are presented in Table 3.

Table 3

Experimental values for roughness parameters R_a and R_q of tested thin films

Sample	Roughness (nm)		
	R_a (nm)	R_q (nm)	Dispersion values
sample 1	0.75	0.95	0.01
sample 2	1.78	2.21	0.02
sample 3	2.13	2.62	0.02

As for the roughness of the film surface of Chromium-Gold sample with 100 nm film thickness of gold, the surface is much smoother because the peak value is 7.50 nm and the valley value is -4.28 nm. Grain size structures do not change a lot and their distribution is somewhat homogeneous. For the roughness of the gold film surface on Cr/SiO₂/Si substrate with 300 nm film thickness of gold, there are some large grains formed and distributed on the film surface. It may be caused by crystallization due to high temperature and relative long sputtering time. The surface is very smooth, so that the peak value and the valley value are similar to those in 100 nm case except at the site of the unexpected large crystals. For the roughness of gold film on Cr/SiO₂/Si substrate with film thickness of 500 nm, the grain is very clear and much larger than those in the above two samples. Also, large crystals can be observed.

One should note that the grain size in films becomes larger when the film thickness increases, which causes the Hall-Petch effect on the flow stress. A sample with larger grain size is able to have more dislocations pipe up, leading to a bigger driving force for dislocations to move from one grain to another. The flow stress increases sharply with grain size. On the other hand, crystallization increases when the film thickness increases. For a range of materials, the increase in yield stress is inversely proportional to the square root of the grain size, and the other quantities follow a similar relationship. This relation, known as the Hall-Petch relation, is well established experimentally from millimeter-sized grains down to the submicron regime [16].

3.2. Effect of nanofilm thickness on adhesion

The force resulting from the molecular interaction between two solids in contact determines adhesion at the contact interfaces. The effective interaction distance between two molecules is known to be finite, which leads to an asymptotical value of the adhesion force between two contacting solids regardless of the thickness of the solids. It can be inferred that, if the thickness of a film in contact with a substrate is less than the effective interaction distance of molecules, the interfacial adhesion force should increase with an increasing film thickness and asymptotically should tend to be constant until a critical film thickness [17].

The force of adhesion between nanoscale rough surfaces was determined from pull-off force measurements made with AFM technique, based on the spectroscopy in point. The AFM tip was brought in contact with the thin film surface and the adhesion force was measured from the pull-off point on the force distance curve. No additional loading force was applied during the point of contact.

The total force of adhesion scaled by the particle radius R can be expressed by Bowden equation (1).

$$F = 2\pi\omega R \left[\frac{R_q}{R + R_q} + \left(\frac{h_c}{h_c + R_q} \right)^2 \right] \quad (1)$$

where R is tip radius in nm (18 nm), R_q is the RMS roughness in μm , h_c is the minimum separating distance between the tip and sample in nm (0.3–0.4 nm) and ω is the work of adhesion in Jm^{-2} .

Based on Johnson, Kendall, and Roberts (JKR-Theory) and Derjaguin, Müller and Toporov (DMT-Theory) a minimum load can be called pull-off force or critical load and it can be determined from equations (2) and (3). In the JKR theory the term of adhesion energy was introduced, in addition to the stored elastic energy of Hertzian contact, which takes into account the effect of adhesion between the two surfaces in contact [18]. For this model, the distribution of the forces of adhesion is reduced to a singular stress when $r = a$ (the contact radius), that is the end of the contact area, and the amount of adhesion force outside the contact is zero [18]. The contact radius between a sphere and a plane with adhesion acting according to the following equation is [19]:

$$a = \left[\frac{R}{K} \left(P + 3\omega\pi R + \sqrt{6\omega\pi R P + (3\omega\pi R)^2} \right) \right]^{1/3} \quad (2)$$

where: P is normal load, R is the radius of the sphere,

$$K = \frac{4}{3} \left(\frac{1 - \nu_1^2}{E_1} + \frac{1 - \nu_2^2}{E_2} \right) \quad (3)$$

E_1 , E_2 are the sphere and flat plane Young's moduli and ν_1 , ν_2 Poisson ratios, respectively.

In the DMT model, according to the elastic Hertz solution both the adhesion force acting outside the contact area (4) and the external load are balanced by the repulsive force within the contact zone; at $r = a$, the stress distribution is not continuous [19], thus:

$$a = \left[\frac{R}{K} (P + 2\omega\pi R) \right]^{1/3} \quad (4)$$

The solution for the adhesive contact between elastic bodies was presented in 1971 by Johnson, Kendall and Roberts (JKR-Theory) and Derjaguin, Müller and Toporov published an alternative adhesive theory in 1975, which is known as the DMT-Theory. The difference between these cases, however, is minor and the JKR-Theory describes adhesion relatively well for flexible spheres, while for small, rigid spheres the DMT-Theory is valid. The assumption of the theory is that the forces of attraction at the contact area are identical to those outside of the area.

That area is reached when the total energy of the system, including the stored elastic energy, the mechanical energy in the applied load and the lost surface energy are in equilibrium. DMT and JKR theories give access to the thermodynamic work of adhesion.

$$F_{C(\text{JKR})} = -\frac{3}{2} \cdot \pi \cdot \omega \cdot R \quad (5)$$

$$F_{C(\text{DMT})} = -2 \cdot \pi \cdot \omega \cdot R \quad (6)$$

In equations (5) and (6), R is the radius of the cantilever tip in nm and ω is interfacial energy of the contact. Quantity of ω can be defined as the work done against the surface attraction in breaking a unit area of the solid-solid interface. On the other hand, is also the work done against the surface attraction when forming a unit area of solid-solid contact and is called the "work of adhesion" per unit area in $\text{J}\cdot\text{m}^{-2}$.

The adhesion force (pull-off force) between the AFM tip and the investigated samples 1, 2 and 3 as well as the snap-in force and adhesion energy are provided by the XEI interpretation software. For instance, Fig.2 presents the experimental spectroscopy in point curves taken on the sample 2. The adhesion force between AFM tip and sample is 136.66 nN (Fig.2) for an ambient condition. The investigated area was divided into 16th equal parts in the form of a square grid which were analyzed and collecting the adhesion forces. More exactly, the first measurement is done and then the tip retracts to its original position. After then the tip moves without contact to the second point of measurement, and so on up to 16 points, without scratching the sample.

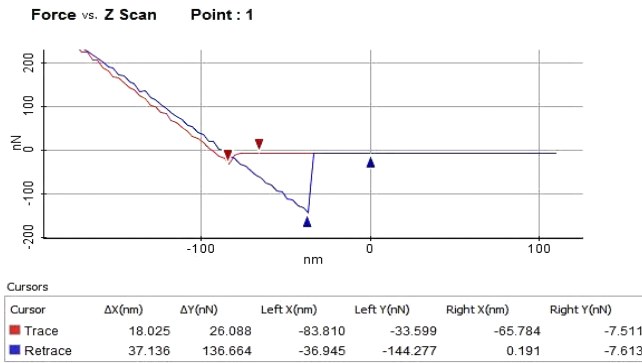


Fig. 2 – Adhesion (pull-off) force between the AFM tip and sample 2.

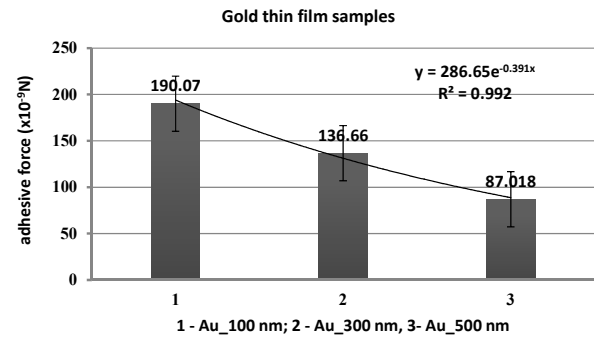


Fig. 3 – Variation of adhesive (pull-off) force as a function of thickness of the samples in ambient environment.

A statistical interpretation of the results was also performed for these data, calculating the dispersion values and the results as presented in Fig. 3.

Cantilevers of spring constant $k = 5.4 \text{ Nm}^{-1}$ were used to cover the complete range of forces measured for all samples, ensuring sufficient lever deflection without excessive instability. This is important for obtaining reliable pull-off forces. Spring constants were not routinely calibrated, and the manufacturer's stated values were assumed. Based on two theories, DMT and JKR expressed by Eqs. (5) and (6) and on the experimental values of the pull-off forces, the work of adhesion was determined. However, the experimental values of pull of forces are somewhat lower than that calculated (144 nN) using a surface energy of $1.7 \text{ J}\cdot\text{m}^{-2}$ for gold [20]. The discrepancy probably arises because there are uncertainties in tip size and geometry.

However, the results for the work of adhesion as a function of thickness of the samples in ambient environment are presented in Table 4.

Table 4

Work of adhesion based on the JKR and DMT theories

Sample	Sample 1	Sample 2	Sample 3
Work of adhesion, ω_{JKR} ($J \cdot m^{-2}$)	2.499	1.515	1.076
Work of adhesion, ω_{DMT} ($J \cdot m^{-2}$)	1.875	1.136	0.807

There was no evidence that variation in speed, contact time, or force limit significantly affected the pull-off force for materials investigated in the paper.

3.3. Effect of nanofilm thickness on friction force

The coefficient of friction was obtained from plots of the lateral force as a function of the applied normal load. To get the friction force between the AFM tip and the sample surface, the sample is scanned by an AFM probe in contact mode. The traces and retrace profiles are stored for each line of the topographic image when a well - defined normal load is applied. The lateral force or friction force is calculated from the difference of these two profiles. The friction force was estimated by the AFM measurements of the d_z rotational deflection of AFM probe results in millivolts (mV).

By considering the sensitivity factor S equal to $97.18 \text{ V}/\mu\text{m}$ for this AFM probe (provided by manufacturer), the rotational deflection can be converted in (nm). The rotational deflections of the AFM cantilever are directly proportional with the friction forces between the AFM tip and investigated samples. The AFM probe type is PPP-LFMR with the following parameters: force constant 0.2 N/m , length $225 \mu\text{m}$, width $48 \mu\text{m}$, thickness $1 \mu\text{m}$, the tip height $15 \mu\text{m}$. Based on torsion beam theory, the friction force between AFM probe and investigated samples acting according to the following equation:

$$F_f = \frac{d_z \cdot r \cdot G \cdot h^3 \cdot b}{l^2 \cdot s} \quad (7)$$

where: d_z is the calibrated deflection of AFM probe [nm], $r=0.33$, G – shear modulus of the AFM cantilever material, l – cantilever length, h – cantilever thickness, b – cantilever width, s – tip height of the AFM probe.

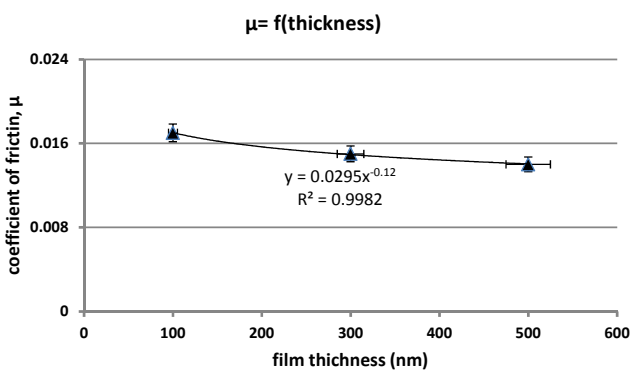


Fig. 4 – Variation of friction coefficient as a function of thickness (load 10 nN, scan rate 0.75 Hz, ambiental conditions).

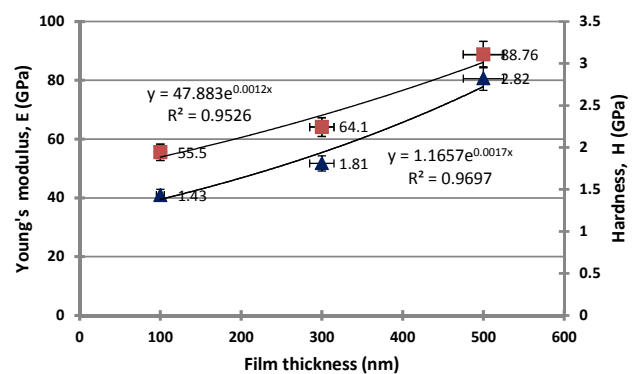


Fig. 5 – Young's modulus E and hardness H versus film thickness.

Figure 4 presents the variation of friction coefficient for investigated thin films as a function of the gold thickness. It can be observed that for a gold film thickness of over 100 nm, the friction coefficient is not largely influenced by the thickness. The coefficient of friction reaches a steady value of approximately 0.015 for gold thin films with thickness larger than 100 nm.

3.4. Effect of nanofilm thickness on mechanical properties

The mechanical properties of the samples were investigated through nanoindentation tests. The hardness (H) of the samples was determined from the load-displacement curve using the Oliver and Pharr method. Young's modulus (E) was evaluated from same curve based on Hertzian contact mode. The Hertz interpretation of the Young's modulus was chosen because the depth of indentation is relatively small. When the indentation depths are smaller than 10 nm, the contact area between the indenter and the thin film is very small and the Young's modulus has a relatively high value for all investigated samples. The indentation force was set at 50 μ N. While H is correlated to the maximum load of the load-displacement curve, E is a function of the slope of the unloading segment.

Considering the indentation size effect, the load of the indenter was chosen to limit the penetration depth less than 10% of the film thickness in order to minimize the effect of substrate on film mechanical properties.

Figure 5 shows the variation of the elastic modulus and hardness for investigated films with thicknesses from 100 nm to 500 nm. The hardness values are ranging from 1.40 GPa to 2.85 GPa and the elastic modulus from 55 GPa to 90 GPa. At 10% of the film thickness a general trend is observed that the nanomechanical properties of samples increase with the film thickness. At 10% of the film thickness, the average curve for the 500 nm gold film shows the highest value ($E=89$ GPa), while the 100 nm gold film exhibits the lowest modulus ($E=55$ GPa). When comparing the hardness values at 10% of the film thickness, the 500 nm gold is the hardest ($H=2.82$ GPa), while the 100 nm gold is the softest ($H=1.43$ GPa).

4. DISCUSSIONS

When the main interest is to understand the nature of material surfaces the surface texture is an important issue. Since crystallization occurs during the manufacturing process, we avoid the indentation testing on large crystals to obtain real values more accurate mechanical characteristics of the investigated film.

It is observed a random dispersion of the values of the pull-off force within a single experiment of about $\pm 5-8$ % on gold surfaces. This is attributed due to combinations of surface quality variations and imperfect balancing of the value of humidity. This was due to the fact that the samples tested clean surfacing became significantly contaminated by the air in the room during the time in which measurements were made.

The adhesion results showed that the adhesion was affected by interactions van der Waals forces, capillary forces and mechanical deformation forces. According to the JKR theory, the adhesion force is affected by the energy of adhesion and the tip radius as shown in equation 2. Therefore, the results shown in Fig.3 are consistent with the JKR model. In this study, the adhesion force increases when the thickness of thin film decreased under the same tip radius.

The friction coefficient values reach a steady value of approximately 0.015 for gold thin films with thickness larger than 100 nm. It was observed that for a thickness of gold thin film over 100 nm, the friction coefficient is not influenced largely by the thickness.

The nanoindentation experiments were used to explore the effect of film thickness on hardness and modulus of elasticity. The discussion is divided into two parts. The first part focuses on the elastic properties of the gold thin films. In the second part, hardness as a function of film thickness is presented. For instance, the precise determination of Young's modulus for samples represents a crucial point for calculating shear stress. The Poisson's ratios of the films and substrates in all the calculations on the experiment data are taken as 0.44, since literature has shown that the Poisson's ratio has a minor effect on the indentation results.

Considering the Hertzian approach, it is observed that the moduli decrease steadily with decreasing of the film thickness. Jarausch et al. found variations in indentation moduli as a function of applied stress for 100 nm gold interconnected films [21]. They found a Young modulus of 48 ± 2 GPa in the absence of stress and 34 ± 2 GPa for 100 MPa total tensile film stress. Furthermore, it was found that around isolated surface steps on a gold (111) sample the elastic modulus varies from 68 ± 1 GPa on the up-step to 72 ± 1 GPa on the down-step. They also concluded that measurements of thin film elastic properties depend strongly on the defect structure (pores and twin boundaries, surface roughness) and the stress state [21].

When analyzing the hardness of Chromium Gold system, the issues are comparable to those described for the modulus. Hardness trends remain unchanged, meaning that, approaching a maximum hardness 2.82 GPa for the 500 nm gold film. The decrease in hardness at 1.43 GPa when the film thickness reaches 100 nm, can be further linked to additional plastic deformation in the substrate of chromium.

Furthermore, the decrease in hardness may also be caused by the difficulties in determining the proper area function for indents smaller than ~ 20 nm. One recent study [22] shows that near the surface, the indentation size effect becomes dominant, and at larger depths a Taylor hardening determines the behavior, which involves the film thickness. Using a Berkovich tip indenter with a radius of 205 nm, Corcoran et al. observed for (100) oriented gold single crystals an increase in hardness as the indentation depth went below 50 nm. They reported values ranging from ~ 0.6 GPa to ~ 2 GPa. Zong and Soboyejo found values for (100) gold hardness between ~ 1 GPa and ~ 1.8 GPa [23,24]. In these cases, as the depth of the indentation is in the range of 50 nm and below, it can be concluded that the effect of indentation size and scaling effects due to film thickness are jointly responsible for the observed behavior.

5. CONCLUSIONS

The paper presents the results of an experimental study on the microstructure and mechanical properties of polycrystalline layers of chromium and gold, with different thickness. The three levels of nominal thickness of gold films are: 100, 300 and 500 nm. The significant conclusions of this work are summarized below.

The grain size of the electron-beam evaporation deposited gold films increase with an increasing film thickness, from approximately 40 nm for the 100 nm thick gold film, to 60 nm for 300 nm thick gold film and 80 nm for the 500 nm thick gold film.

From experimental evaluation of surface roughness for the investigated samples we observed that: the R_a value is approximately 0.75nm for the 100 nm thick gold film, 1.75–1.80 nm for 300 nm thick gold film and around 2.10–2.5 nm for the 500 nm thick gold film.

If the thickness of a film in contact with a substrate is less than the effective interaction distance of molecules, the interfacial adhesion force should increase with an increasing film thickness and asymptotically should tend to be constant until a critical film thickness. Based on two theories, DMT and JKR and on the experimental values of the pull-off forces was determined the work of adhesion, which is between 1 and 2.5 Jm^{-2} , decreasing if the thickness film layer increases. The coefficient of friction was obtained from plots of the lateral force for the applied normal load. It can be observed that over 100 nm thickness of film the friction coefficient is not largely influenced by the thickness. The coefficient of friction reaches a steady value of approximately 0.015 for gold thin films with thickness larger than 100 nm.

In terms of elastic properties, the accurate determination of the indentation modulus was difficult because of the small volumes which were probed. The hardness and elastic modulus of the gold thin film with different thickness was measured using a nanoindenter. The hardness values are ranging from 1.40 GPa to 2.85 GPa and the elastic modulus from 55 GPa to 90 GPa. A general trend is observed that the nanomechanical properties of the Chromium-Gold increase with the film thickness. The general rules when testing mechanical properties of thin films is to indent only the first 10-20 % of the film thickness to avoid the substrate effect on measurements.

ACKNOWLEDGMENTS

This work was supported by the Romanian Space Agency – STAR Project no. 193 / 2017, grant from the Research Program for Space Technology Development and Innovation and Advanced Research (STAR).

REFERENCES

1. K. MONGKOLSUTTIRAT, *Mechanical properties and resistivity of gold and gold-vanadium oxide thin films*, Degree of Master of Science, Lehigh University, ProQuest Dissertations Publishing, 2009.
2. R. MABOUDIAN, W.R. ASHURST, C. CARRARO, *Tribological challenges in micromechanical systems*. Tribol Lett, **12**, 2, pp. 95–100, 2002, <https://doi.org/10.1023/A:1014044207344>.

3. S.M. HSU, *Nano-lubrication: concept and design*. Tribol Int, **37**, 7, pp. 537–545, 2004, <https://doi.org/10.1016/j.triboint.2003.12.002>.
4. B. BHUSHAN, *Handbook of micro/nano tribology*, CRC press, 1998.
5. R.C. VOICU, M. PUSTAN, C. BIRLEANU, A. BARACU, R. MULLER, *Mechanical and tribological properties of thin films under changes of temperature conditions*. Surf Coat Technol, **271**, pp. 48–56, 2015, <https://doi.org/10.1016/j.surfcoat.2015.01.026>.
6. C. BIRLEANU, M. PUSTAN, R. MULLER, C. DUDESCU, V. MERIE, R.C. VOICU, A., BARACU, *Experimental investigation by atomic force microscopy on mechanical and tribological properties of thin films*, Int J Mater Res, **107**, 5, pp. 429–438, 2015, <https://doi.org/10.3139/146.111358>.
7. D.S. GHOSH, *Ultrathin metal transparent electrodes for the optoelectronics industry*, Doctoral thesis, Universitat Politècnica de Catalunya, 2012.
8. K. MONGKOLSUTTIRAT, *Time and temperature dependence of viscoelastic stress relaxation in Au and Au alloy thin films*. Degree of Doctor of Philosophy, Lehigh University, ProQuest Dissertations Publishing, 2013.
9. A. CHAU, S. REGNIER, A. DELCHAMBRE, P. LAMBERT, *Theoretical and experimental study of the influence of AFM tip geometry and orientation on capillary force*, Journal of Adhesion Science and Technology, **24**, 15-16, pp. 2499–2510, 2010, <https://doi.org/10.1163/016942410X508307>.
10. V. BELLITTO, *Atomic Force Microscopy – imaging, measuring and manipulating surfaces at the atomic scale*, published online: Intech, 2012.
11. M. PALACIO, B. BHUSHAN, *Ultrathin wear-resistant ionic liquid films for novel MEMS/NEMS applications*, Adv Mater, **20**, 6, 2008, pp. 1194–1198, DOI:10.1002/adma.200702006.
12. AGILENT, Application note: *Nanotribology of hard thin film coatings: A case study using the G200 nanoindenter*.
13. B. MERLE, *Mechanical properties of thin films studied by bulge testing*, FAU University Press, 2013.
14. J. VANCEA, G. REISS, F. SCHNEIDER, K. BAUER, H. HOFMANN, *Substrate effects on the surface topography of evaporated gold films – a scanning tunnelling microscopy investigation*, Surface science, **218**, 1, pp. 108–126, 1989, [https://doi.org/10.1016/0039-6028\(89\)90622-5](https://doi.org/10.1016/0039-6028(89)90622-5).
15. J.B. CHANG, V. SUBRAMANIAN, *Effect of active layer thickness on bias stress effect in pentacene thin-film transistors*. Appl. Phys. Lett, **88**, 23, p. 233513, 2006, <https://doi.org/10.1063/1.2210791>.
16. J. SCHIÖTZ, K.W. JACOBSEN, *A maximum in the strength of nanocrystalline copper*, Science, **301**, 5638, pp. 1357–1359, 2003, DOI: 10.1126/science.1086636.
17. Z. PENG, S. CHEN, *Effects of surface roughness and film thickness on the adhesion of a bioinspired nanofilm*, Phys. Rev. E, **83**, 5, p. 051915, 2011, <https://doi.org/10.1103/PhysRevE.83.051915>.
18. D. XU, K.M. LIECHTI, K. RAVI-CHANDAR, *On the modified Tabor parameter for the JKR–DMT transition in the presence of a liquid meniscus*, J Colloid Interface Sci, **315**, 2, pp. 772–785, 2007, <https://doi.org/10.1016/j.jcis.2007.07.048>.
19. D. GRIERSON, E. FLATER, R. CARPICK, *Accounting for the JKR–DMT transition in adhesion and friction measurements with atomic force microscopy*, J Adhes Sci Technol, **19**, 3-5, pp. 291–311, 2005, <https://doi.org/10.1163/1568561054352685>.
20. R. JONES, H.M. POLLOCK, J.A.S. CLEAVER, C.S. HODGES, *Adhesion forces between glass and silicon surfaces in air studied by AFM: Effects of relative humidity, particle size, roughness, and surface treatment*, Langmuir, **18**, 21, pp 8045–8055, 2002, DOI: 10.1021/la0259196.
21. K. JARAUSCH, J.D. KIELY, J.E. HOUSTON, P.E. RUSSELL, *Defect-dependent elasticity: nanoindentation as a probe of stress state*, J. Mater. Res, **15**, 8, pp. 1693–1701, 2000, <https://doi.org/10.1557/JMR.2000.0244>.
22. M. CORDILL, D.M. HALLMAN, N.R. MOODY, D.P. ADAMS, W.W. GERBERICH, *Thickness effects on the plasticity of gold films*, Metall and Mat Trans A., **38**, 13, pp. 2154–2159, 2007, <https://doi.org/10.1007/s11661-006-9011-7>.
23. Y. CAO, S. ALLAMEH, D. NANKIVIL, T.S. SATHIARAJ, T. OTITI, W. SOBOYEJO, *Nanoindentation measurements of the mechanical properties of polycrystalline Au and Ag thin films on silicon substrates: Effects of grain size and film thickness*. Mater Sci Eng A, **427**, 1, pp. 232–240, 2006, <https://doi.org/10.1016/j.msea.2006.04.080>.
24. Z. ZONG, W. SOBOYEJO, *Indentation size effects in face centered cubic single crystal thin films*, Mater Sci Eng: A, **404**, 1, pp. 281–290, 2005, <https://doi.org/10.1016/j.msea.2005.05.075>.

Received September 20, 2018